Available online at www.sciencedirect.com
ScienceDirect
Bioorganic & Medicinal Chemistry Letters
Bioorganic & Medicinal Chemistry Letters 17 (2007) 3266–3270

# 4-Aryl-5-cyano-2-aminopyrimidines as VEGF-R2 inhibitors: Synthesis and biological evaluation

Terry V. Hughes,[a,*] Stuart L. Emanuel,[a] Amanda K. Beck,[a] Steven K. Wetter,[a] Peter J. Connolly,[a] Prabha Karnachi,[a] Michael Reuman,[a] Jabed Seraj,[a] Angel R. Fuentes-Pesquera,[a] Robert H. Gruninger,[a] Steven A. Middleton,[a] Ronghui Lin,[a] Jeremy M. Davis[b] and David F. C. Moffat[b]

[a]*Johnson & Johnson Pharmaceutical Research and Development, L.L.C, PO Box 300, 1000 Route 202, Raritan, NJ 08869, USA*
[b]*UCB Pharma, 216 Bath Road, Slough SL14EN, UK*

Received 3 February 2007; revised 1 April 2007; accepted 4 April 2007
Available online 10 April 2007

**Abstract**—A novel series of 4-aryl-5-cyano-2-aminopyrimidines were synthesized and found to have potent VEGF-R2 kinase inhibitory activity. Structure–activity relationships were investigated and compound **14a** was shown to be efficacious in a mouse model of corneal neovascularization.


Angiogenesis is the formation of new blood vessels, and is an essential process for tumor growth. The selective inhibition of tumor angiogenesis might be a useful strategy for inhibiting tumor growth and metastasis. Pathological angiogenesis in the retina is a major cause of blindness and is responsible for the deterioration of vision that occurs in diabetic retinopathy, age-related macular degeneration, and retinopathy of prematurity. Several growth factors are elevated in the eye of patients with active neovascularization that contribute to the formation of new vessels.[1,2] Vascular endothelial growth factor (VEGF) and basic fibroblast growth factor (bFGF) are critical components in the development of pathological angiogenesis and are involved in the etiology of these diseases. VEGF stimulates ocular neovascularization, increases vascular permeability, and correlates with disease progression.[3] This makes the VEGF signal transduction pathway an attractive target for therapeutic intervention in ischemic ocular disease. We have discovered a series of potent VEGF-R2 kinase inhibitors that are potentially useful as anti-angiogenesis agents for the treatment of cancer and diabetic retinopathy. We recently reported the in vitro anti-angiogenic, in vivo anti-tumor activity of **14a** (JNJ-17029259) as well as its activity against VEGF-R2 and other biologically relevant kinases.[4] Herein, we report the SAR development, synthesis, and biological activity of 4-aryl-5-cyano-2-aminopyrimidines that display potent inhibition of VEGF-R2 kinase.[5] We also describe the proposed binding mode of the pharmacophore and the rationale for structure–activity relationships.

Routine screening for selective VEGF-R2 inhibitors provided compound **1** (Scheme 1) as a hit with VEGF-R2 $IC_{50} = 1.0\ \mu M$ and cyclin-dependent kinase-1 (CDK1) $IC_{50} > 100\ \mu M$.

Compound **1** was docked into a homology model of VEGF-R2 using the software GLIDE.[6,7] The proposed binding mode (Fig. 2) shows the top reranked pose of the ligand as overlapped with ATP along with the binding pockets of the ATP site.[8] The amino pyrimidine forms hydrogen bonds with backbone C=O and NH of CYS 917 in the hinge region in the ATP site. The cyano group is positioned at the opening of the hydrophobic pocket.

Synthesis of 4-substituted-5-cyano-2-aminopyrimidines (**2**) is outlined in Scheme 2. The key step involved reaction of a vinylogous amide with a guanidinium salt to form the pyrimidine ring. Specifically, conversion of an

*Keywords*: VEGF-R2; Kinase; KDR; Cancer; Angiogenesis; Kinase inhibitor; 2-Aminopyrimidines.
* Corresponding author. E-mail: hughe007@hotmail.com

0960-894X/$ - see front matter © 2007 Elsevier Ltd. All rights reserved.
doi:10.1016/j.bmcl.2007.04.021

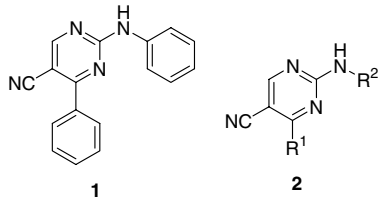

**Scheme 1.** Screening hit compound **1** and general structure of pharmacophore **2**.

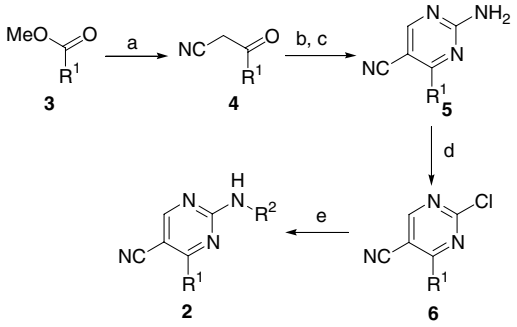

**Scheme 2.** Reagents and conditions: (a) *n*-BuLi, $CH_3CN$, THF, −78 to −45 °C (80–100%); (b) DMF-DEA, DMF, 25 °C; (c) guanidine nitrate, DMF, $NaHCO_3$ (92%, over 2 steps); (d) $SbCl_3$, *tert*-butyl nitrite, 1,2-dichloroethane, 25 °C (47%); (e) $R^2NH_2$, THF, 25 °C to reflux, $NaHCO_3$ (73–95%).

aryl methyl ester **3** ($R^1$ = aryl) to the corresponding α-cyanoketone **4** was achieved via formation of the lithium salt of acetonitrile by treatment with *n*-BuLi at −78 °C followed by reaction with the ester **3** at −45 °C. Subsequent treatment of the α-cyanoketone **4** with *N*,*N*-dimethylformamide diethyl acetal (DMF-DEA) formed a vinylogous amide in situ that was reacted with guanidine nitrate in DMF at 100 °C to form the 2-amino-4-aryl-5-cyanopyrimidine **5**. The Sandmeyer reaction of the aminopyrimidine **5** was accomplished by treatment with antimony trichloride and *tert*-butylnitrite in 1,2-dichloroethane at 25 °C to smoothly afford the 2-chloropyrimidine **6**.[9] The displacement of the Cl of **6** with aliphatic amines proceeded at 25 °C and with aromatic amines in refluxing THF to afford the pharmacophore **2**. The synthesis of analogues via Scheme 2 was divergent and allowed for the late stage modification of $R^2$. Initial exploration of the SAR of the $R^2$ substituent was determined by reacting 2-chloro-5-cyano-4-phenylpyrimidine **6** ($R^1$ = phenyl) with more than 65 different amines. The VEGF-R2 and CDK1 enzyme inhibitory activities of representative analogues are summarized in Table 1.

A second synthetic route, outlined in Scheme 3, is convergent and relies on the synthesis of different guanidine salts **8** to vary the $R^2$ substituent. The guanidine salts **8** were synthesized by reacting amines **7** with cyanamide and 12 N HCl in refluxing EtOH.[5] The α-cyanoketone **4** was treated with DMF-DEA in DMF at 25 °C and the resulting vinylogous amide was reacted with the guanidine salt **8** and $NaHCO_3$ at 100 °C in a one-pot reaction to yield analogues **2**. Analogues where $R^1$ was electron rich (e.g., indolyl, pyrrolyl) were synthesized via Scheme 3 as they were not stable to the Sandmeyer conditions outlined in Scheme 2.

Examination of the $R^2$ substituent data revealed that electron-donating substituents such as alkyl or methoxy (**2g**, **i**, **j**) are tolerated at the *para* and *meta* positions, but VEGF-R2 activity is considerably reduced with an electron-withdrawing chloride (**2o**). Substitution at the *ortho* position also results in loss of kinase activity, possibly due to unfavorable steric interactions (**2n**,**p**). Analogues having heteroaromatic rings such as pyrimidine (**2m**) or benzimidazole (**2l**) directly attached to the 2-amino group were poor VEGF-R2 inhibitors. However, the indol-5-yl derivative **2h**, which is attached to the 2-amino group through the benzene ring, was about twice as potent as the parent compound **1**. Interestingly, **2h** was 4-fold more potent than the all-carbon naphthalen-2-yl analogue **2k**, consistent with the trend toward enhanced kinase potency with electron-rich ring systems. Expanding on the favorable *para*-alkyl substitution pattern, the attachment of polar groups to the alkyl chain led to analogues with improved kinase potency. Thus, hydroxyl substitution on the *para*-alkyl group (**2f**) resulted in an increase in VEGF-R2 potency compared to **2j**, and amine substitution increased potency even more (**2a**–**c**). Attachment of the amino group via a 1-carbon linker (**2a**) displayed similar activity when compared to the same group attached by a 2-carbon linker (**2c**). The meta aminoalkyl analogue **2e** and the morpholine amide **2d** were somewhat weaker VEGF-R2 inhibitors than the preferred para aminoalkyl compounds.

With SAR for $R^2$ groups in hand, we fixed $R^2$ and varied $R^1$. Several analogues with various $R^1$ groups were made via the synthesis of specific arylguanidines **8** as detailed in Scheme 3. Table 2 details a representative selection of analogues **9** made with $R^2$ fixed as 4-(2-hydroxyethyl)phenyl. A variety of aromatic and heteroaromatic rings was tolerated at $R^1$ but the *tert*-butyl (**9j**) and indol-2-yl (**9i**) groups led to significant loss of kinase potency. Some of the better substituents for VEGF-R2 kinase inhibition such as 4-(2-amino-2-propyl)phenyl (**9a**) and indol-5-yl (**9c**) contained an NH group capable of acting as an H-bond donor. Molecular modeling indicated that the $NH_2$ of **9a** and the NH of **9c** participate in a favorable H-bond with the backbone C=O of Arg 177 in the phosphate binding site.

Next, the hydroxyl groups of **9** were transformed into pendant amino groups via mesylation and displacement with an amine or via oxidation and reductive amination to afford the 1 and 2-carbon linked analogues **10** as detailed in Scheme 4. Numerous analogues **14**, where $R^1$ is fixed as 4-(2-amino-2-propyl)phenyl and $R^2$ is varied, were synthesized to optimize inhibition of VEGF-R2 kinase (Scheme 5).[10] Some examples of the VEGF-R2 activity of analogues **14** are shown in Table 3. All analogues were selective for VEGF-R2 and had greatly reduced potency against CDK1. Notably, compound **14a** was a very potent VEGF-R2 kinase inhibitor with an $IC_{50}$ value of 27 nM. *Para*-substitution (**14a**) was shown

**Table 1.** SAR for $R^2$ substituent of compounds **1** and **2a**–**p** ($R^1$ = Ph)

| Compound | $R^2$ | VEGF-R2 $IC_{50}$[a] (μM) | CDK1 $IC_{50}$[a] (μM) |
|---|---|---|---|
| **1** | Phenyl | 1.0 | >10 |
| **2a** | 4-(Pyrrolidin-1-yl-$CH_2$)phenyl | 0.061 | 6.2 |
| **2b** | 3-Methoxy-4-(pyrrolidin-1-yl-$CH_2$)phenyl | 0.091 | 9.0 |
| **2c** | 4-(Pyrrolidin-1-yl-$CH_2CH_2$)phenyl | 0.11 | 6.5 |
| **2d** | 4-(3-Morpholin-4-yl-3-oxopropyl)phenyl | 0.18 | 2.1 |
| **2e** | 3-(Morpholin-4-yl-$CH_2$)phenyl | 0.36 | 2.0 |
| **2f** | 4-(2-Hydroxyethyl)phenyl | 0.20 | 2.0 |
| **2g** | 3-Methoxyphenyl | 0.38 | 4.2 |
| **2h** | 2-Methylindol-5-yl | 0.41 | 3.3 |
| **2i** | 4-Methoxyphenyl | 0.49 | 3.3 |
| **2j** | 4-Methylphenyl | 1 | 3.5 |
| **2k** | Naphthalen-2-yl | 2.1 | >10 |
| **2l** | Benzimidazol-2-yl | 10 | >10 |
| **2m** | Pyrimidin-2-yl | >10 | >10 |
| **2n** | 2-Chlorophenyl | >10 | >10 |
| **2o** | 4-Chlorophenyl | >10 | >10 |
| **2p** | 2-Methoxyphenyl | >10 | >10 |

[a] $IC_{50}$ data are the average of at least two separate experiments. $IC_{50}$ values listed as >10 indicate no observed 50% inhibition at 10 μM, nor was an inhibition maximum observed. Assay performed at 5 μM ATP concentration.

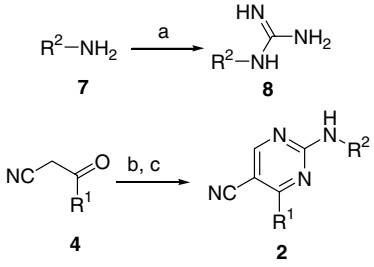


**Scheme 3.** Reagents and conditions: (a) cyanamide, 12 N HCl, EtOH, reflux (78%); (b) DMF-DEA, DMF, 25 °C; (c) **8**, DMF, $NaHCO_3$, 100 °C (60%).

**Table 2.** SAR for $R^1$ substituent for analogues **9** ($R^2$ = 4-$HO(CH_2)_n$Ph)

| Compound | *n* | $R^1$ | VEGF-R2 $IC_{50}$[a] (μM) | CDK1 $IC_{50}$[a] (μM) |
|---|---|---|---|---|
| **9a** | 2 | 4-(2-Amino-2-propyl) phenyl | 0.052 | 1.6 |
| **9b** | 2 | 2-Thienyl | 0.082 | 0.47 |
| **9c** | 2 | 5-Indolyl | 0.090 | 0.41 |
| **9d** | 2 | 4-Methoxyphenyl | 0.15 | 1.5 |
| **9e** | 2 | 4-Bromophenyl | 0.18 | 2.0 |
| **9f** | 2 | 4-Sulfamoylphenyl | 0.20 | 1.9 |
| **9g** | 2 | Benzothiazol-2-yl | 0.34 | 0.56 |
| **9h** | 2 | 4-(2-Hydroxy-2-propyl) phenyl | 0.41 | 2.7 |
| **9i** | 2 | Indol-2-yl | 1.4 | 1.7 |
| **9j** | 2 | *tert*-butyl | 1.6 | 1.1 |

[a] $IC_{50}$ data are the average of at least two separate experiments. Assay performed at 5 μM ATP concentration.

to confer better potency than *meta*-substitution (**14b**). Compound **14e**, which has an oxygen inserted in the linker, was shown to be 20-fold less potent against VEGF-R2 than **14a**.[11]

*Corneal micropocket model.*[12,13] The VEGFR-2 inhibitor (SU-5416) has been reported in the literature to have

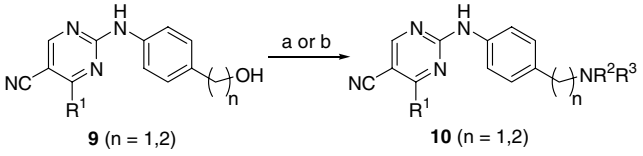


**Scheme 4.** Reagents and conditions: (a) $CH_3SO_2Cl$, $Et_3N$, 0–25 °C; $NHR^1R^2$, DMF, 70 °C (73%); (b) Dess-Martin periodinane, THF, 25 °C; $NHR^1R^2$, $NaHB(OAc)_3$, THF, 25 °C.

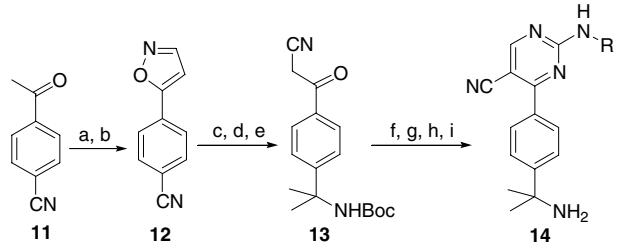


**Scheme 5.** Reagents and conditions: (a) DMF-DEA, DMF, 25 °C; (b) $NH_2OH{\cdot}HCl$, MeOH, 25 °C (75%); (c) powdered $CeCl_3$, MeLi, 25 °C, sonication; (d) $BOC_2O$, toluene, reflux (82%); (e) NaOH, EtOH, 25 °C (92%); (f) DMF-DEA, DMF, 25 °C; (g) *N*-[4-(2-hydroxyethyl)phenyl]-guanidine nitrate, DMF, $NaHCO_3$, 100 °C (83%); (h) $CH_3SO_2Cl$, $Et_3N$, 0–25 °C; (i) $NH_2R$, DMF, 70 °C (65%); (j) TFA, DCM, then $K_2CO_3$ (95%).

inhibited neovascularization in a corneal pocket model.[14] To investigate if the antiangiogenic effects of these analogues would translate to efficacy in animal models of retinopathy, compound **14a** was evaluated in mice in a corneal micropocket model for inhibition of growth factor-induced neovascularization in the eye as described (Fig. 1). A marked reduction in vessel growth was observed at all doses following oral administration of compound **14a**. Although the 100 mg/kg dose reduced vessel growth, the effects at this dose only approached the cutoff for significance ($p = 0.059$). Compound **14a**

**Table 3.** SAR for R substituent for analogues **14**

| Compound | R | VEGF-R2 $IC_{50}$[a] (μM) | CDK1 $IC_{50}$[a] (μM) |
|---|---|---|---|
| **14a** | 4-(Morpholin-4-yl-$CH_2CH_2$)phenyl | 0.027 | 4.1 |
| **14b** | 3-(Morpholin-4-yl-$CH_2CH_2$)phenyl | 0.055 | 5.7 |
| **14c** | 4-(2-Ethylimidazol-1-yl-$CH_2CH_2$)phenyl | 0.094 | 4.8 |
| **14d** | 4-(4-Methylpiperazin-1-yl-$CH_2CH_2$)phenyl | 0.021 | 5.6 |
| **14e** | 4-(Morpholin-4-yl-$CH_2CH_2O$)phenyl | 0.45 | 21 |

[a] $IC_{50}$ data are the average of at least two separate experiments. Assay performed at 5 μM ATP concentration.

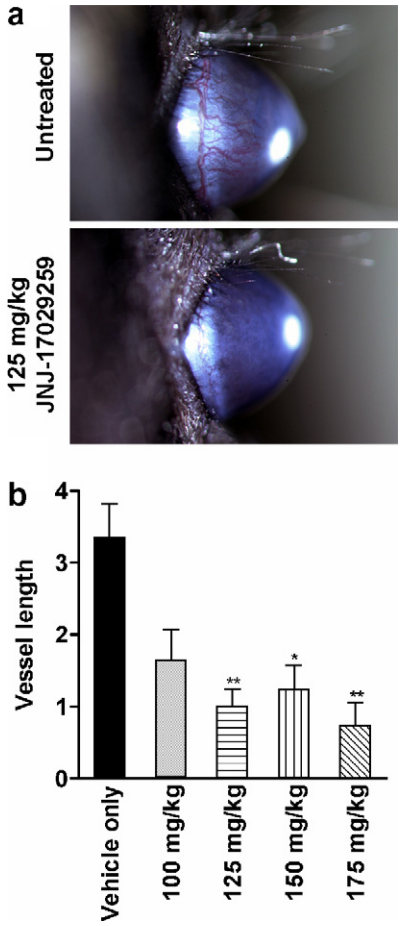


**Figure 1.** Corneal micropocket assay. Pellets containing bFGF were implanted in one eye of C57BL6 mice to induce a vascular response. (a) Representative photos of neovascularization induced by pellets containing bFGF and dosed with 0.5% methylcellulose (vehicle) or 125 mg/kg compound **14a**. (b) Inhibition of bFGF-induced retinal neovascularization by compound **14a** was assessed in mice following daily oral administration for 6 days at the indicated dose levels. Results are expressed as total vessel length in mm. Bars, SE; $^{*}p < 0.05$, $^{**}p < 0.01$, compared to the vehicle + bFGF positive control group by one-way ANOVA with Dunnett's post hoc test.

was orally available in nude mice (44 %F, AUC = 15.6 μM-h, dose = 3 mg/Kg). The plasma levels of **14a** reach 12 μM with a $t_{1/2}$ of 7 h with an oral dose of 100 mg/kg in nude mice. Doses of 125 mg/kg and above resulted in statistically significant reductions in neovascularization relative to the animals dosed with vehicle alone. Compound **14a** was efficacious at inhibiting corneal neovascularization at several doses and daily oral therapy was well tolerated with no decrease in body weight and no treatment-related deaths.

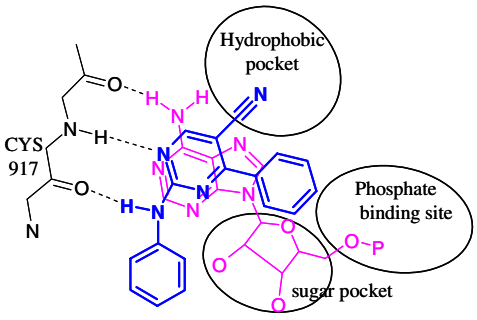


**Figure 2.** Proposed binding mode of compound **1** in the active site of VEGF-R2 as overlapped with ATP.

In summary, we have described the SAR development and synthesis of a novel series of 4-aryl-5-cyano-2-aminopyrimidines that are potent and selective inhibitors of VEGF-R2. The SAR development for $R^2$ of the pharmacophore **1** relied upon a divergent synthesis (Scheme 2), while the SAR optimization for $R^1$ focused on a more convergent approach (Scheme 3). Compound **14a** displayed potent inhibition of VEGF-R2 in vitro and was shown to be orally efficacious at inhibiting corneal neovascularization in vivo. Interfering with the VEGF signal transduction pathway with pharmacological agents represents a potential method for reducing or preventing vision loss associated with uncontrolled retinal angiogenesis.

## References and notes

1. Aiello, L. P.; Avery, R. L.; Arrigg, P. G.; Keyt, B. A.; Jampel, H. D.; Shah, S. T.; Pasquale, L. R.; Thieme, H.; Iwamoto, M. A.; Park, J. E.; Nguyen, H. V.; Aiello, L. M.; Ferrara, N.; Park, G. L. *New Engl. J. Med.* **1994**, 1480.
2. Adamis, A. P.; Miller, J. W.; Bernal, M. T.; D'Amico, D. J.; Folkman, J.; Yeo, T. K.; Yeo, K. T. *Am. J. Opthamol.* **1994**, 445.
3. Ozaki, H.; Seo, M.-S.; Ozaki, K.; Yamada, H.; Yamada, E.; Okamoto, N.; Hofmann, F.; Wood, J. M.; Campochiaro, P. A. *Am. J. Pathol.* **2000**, 697.
4. Emanuel, S.; Gruninger, R. H.; Fuentes-Pesquera, A.; Connolly, P. J.; Seamon, J. A.; Hazel, S.; Tominovich, R.; Hollister, B.; Napier, C.; D'Andrea, M. R.; Reuman, M.; Bignan, G.; Tuman, R.; Johnson, D.; Moffatt, D.; Batchelor, M.; Foley, A.; O'Connell, J.; Allen, R.; Perry, M.; Jolliffe, L.; Middleton, S. A. *Mol. Pharmacol.* **2004**, *66*, 635.
5. Batchelor, M. J.; Moffat, D. F. C.; Davis, J. M.; Hutchings, M. C. U.S. Patent 6,579,983, 2003.
6. Glide 3.5, Schrodinger, New York, 2005.
7. (a) Friesner, R. A.; Banks, J. L.; Murphy, R. B.; Halgren, T. A.; Klicic, J. J.; Mainz, D. T.; Repasky, M. P.; Knoll, E. H.; Shaw, D. E.; Shelley, M.; Perry, J. K.; Francis, P.; Shenkin, P. S. *J. Med. Chem.* **2004**, 1739; (b) Doe, J. S.; Smith, J. J.; Roe, R. P. *J. Am. Chem. Soc.* **1968**, 8234.

8. No scaling factors were applied to the van der Waals radii. Default settings were used for all the remaining parameters. The top 20 poses based on Glidescore were energy-minimized with Macromodel using both the OPLS-AA, and the refined poses reranked using Glidescore.
9. Liu, M.; Luo, M.; Mozdziesz, D. E.; Sartorelli, A. C. *Nucleosides Nucleotides* **2005**, 45.
10. Details of the synthetic transformation of **11**–**14** will be reported elsewhere.
11. More than 40 potent and selective VEGF-R2 kinase inhibitors from the 4-aryl-5-cyano-2-aminopyrimidine series were tested in an A375 in vivo xenograft tumor model in nude mice. While most compounds displayed good oral efficacy, compound **14a** was the most efficacious analogue at suppressing tumor growth.[4]
12. Kenyon, B. M.; Voest, E. E.; Chen, C. C.; Folkman, J.; D'Amato, R. J. *Investig. Ophtalmol. Vis. Sci.* **1996**, *37*, 1625.
13. Angiogenesis was induced with bFGF in these models because it produced a more robust vascular response than VEGF (data not shown).
14. Hirata, A.; Ogawa, S.-I.; Komentani, T.; Kuwano, T.; Naito, S.; Kuwano, M.; Ono, M. *Cancer Res.* **2002**, 2554.